Order Parameters and Carbon Shielding Tensors of Some Anthracene Derivatives from 13C NMR Experiments

ARTICLE *in* THE JOURNAL OF PHYSICAL CHEMISTRY · OCTOBER 1996

Impact Factor: 2.78 · DOI: 10.1021/jp962052+

Order Parameters and Carbon Shielding Tensors of Some Anthracene Derivatives from ^{13}C NMR Experiments

Riccardo Tarroni and Claudio Zannoni*

Dipartimento di Chimica Fisica ed Inorganica, Università degli Studi di Bologna, Viale Risorgimento 4, 40136 Bologna, Italy

Received: July 10, 1996[⊗]

The orientational order parameters and approximate ^{13}C shielding tensors of anthracene and of six of its 9,10-derivatives, 9,10-dihydroanthracene, 9,10-dimethylanthracene, 9,10-dibromoanthracene, anthraquinone, 9,10-diphenylanthracene, and 9,10-*bis*(phenylethynyl)anthracene, dissolved in the nematic liquid crystal ZLI-1167 have been determined using a recently proposed ^{13}C NMR method. The biaxial order parameters obtained are compared with some current theoretical models of ordering. We find that none of these mean field approaches have fully satisfactory predictive capabilities.

1. Introduction

A nonspherical solute dissolved in a nematic liquid crystal becomes partially ordered with respect to the preferred direction of the solvent and its orientational distribution, and the probability $P(\omega)$ of finding the solute molecule at a certain orientation, ω, becomes anisotropic. This solute alignment is at the heart of many liquid crystal applications, for instance of dye-based displays[1] and the use of liquid crystal solvents in spectroscopy.[2] On a more fundamental level the ordering of suitably chosen solutes can offer a handle for the understanding of intermolecular anisotropic interactions in liquid crystals. Indeed it is not completely clear at present how important factors like anisotropic steric repulsion or attractive dispersive forces are in determining molecular ordering. The theories available, mostly of the molecular field type, try to predict ordering starting from a certain selected molecular feature, e.g. shape or polarizability and its associated anisotropy and biaxiality.[3−5]

An appropriate testing of these theories requires the availability of order parameters and of their temperature dependence for sets of simple molecules, possibly with a well-defined symmetry and a clear trend of variation in their shape or in some other relevant property, such as their polarizability.

Surprisingly enough not a great amount of such series is available. Most data are obtained from deuterium NMR (DNMR),[6,7] and the difficulty often associated with isotopic substitution can at least partly explain the lack of extensive sets of order parameter data.

We have recently developed a method for determining ordering matrices from natural abundance ^{13}C NMR measurements,[8] and we have tested it on a number of simple aromatics dissolved in the liquid crystal ZLI-1167, a ternary mixture of aliphatic mesogenic cyanocyclohexyls. In particular we have shown that the method can be used to obtain, in a relatively simple way, order parameters of quality comparable to those obtained with DNMR over a wide temperature range.

Here we apply this ^{13}C technique to the determination of the ordering matrix for various anthracenes substituted in the same positions, as discussed in section 2 and 3. Then we compare the results with the predictions of various models put forward in the literature: the elastic continuum model,[3] the dispersive interactions model,[4] and the surface tensor model.[5] Each of these approaches can predict the ordering biaxiality starting from a certain molecular property, that is in turn assumed to be at the origin of the solute molecular alignment. These properties follow from molecular shape in different ways for the continuum and the surface models, and from polarizability for the dispersive model, and we evaluate them for the molecules we present, finding the respective biaxialities.

2. Experimental Section

Anthracene (ANTH), 9,10-dihydroanthracene (DHYA), 9,-10-dimethylanthracene (DMEA), 9,10-dibromoanthracene (DBRA), anthraquinone (ATQN), 9,10-diphenylanthracene (DPHA) and 9,10-bis(phenylethynyl)anthracene (DPEA) were purchased from Aldrich and used without further purification. The liquid crystal ZLI-1167, a ternary eutectic mixture of aliphatic mesogens (4′-propyl-, 4′-pentyl-, and 4′-heptyl-4-cyanobicyclohexyls),[9] was purchased from Merck.

Each sample was prepared by sealing the liquid crystal solvent and the molecular probe in a NMR tube 8 mm in diameter at approximately 3% w/w concentration; the probes dissolve completely at this concentration, except for DPEA and particularly ATQN.

The temperature-dependent series of ^{13}C NMR spectra were recorded on a Bruker CXP 300 spectrometer, using the same experimental setup and procedure described in ref 8, hereafter referred as I. At least 400 scans were accumulated at each temperature. For ATQN up to 3000 scans were required to achieve a sufficiently high signal to noise ratio.

In Figures 1−7 we show the observed chemical shifts, the labeling of the carbons, and the line assignments both in isotropic and in nematic phase. For the isotropic line assignments we essentially resorted to literature data,[10−12] while for the assignments in the mesophase we applied the iterative trial-and-error procedure described in I. In Figures 1−7 the line shifts are referred to the frequency of the −CN line in the isotropic phase. This is possible because all the spectra were collected in a single-temperature sweep, without removing the sample from the probe-head. This way of presenting the results gives a useful representation of the appearance of the spectra and of their temperature variation.

3. Data Analysis

The procedure adopted to analyze the temperature-dependent ^{13}C spectra was described in detail and validated against known

[⊗] Abstract published in *Advance ACS Abstracts,* September 15, 1996.

S0022-3654(96)02052-7 CCC: $12.00

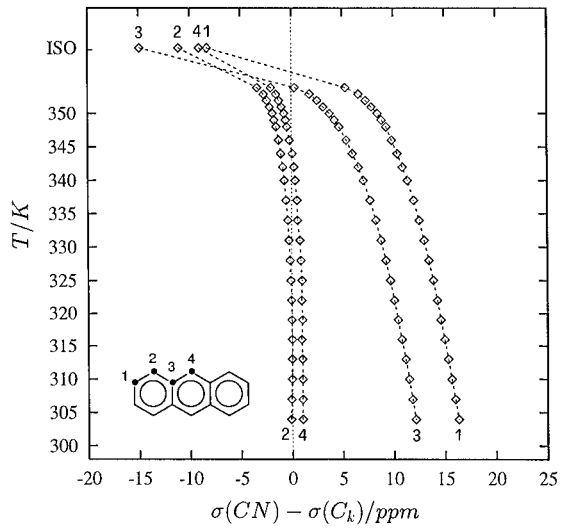

Figure 1. Temperature dependence and assignments of the chemical shifts (ppm) of anthracene (ANTH) in isotropic and nematic phases of ZLI-1167, referred to the chemical shift of the −CN group of the liquid crystal in the isotropic phase. Dashed lines connect the peaks belonging to the same carbon at the various temperatures. The nematic/isotropic transition temperature T_{NI} is 354 K.

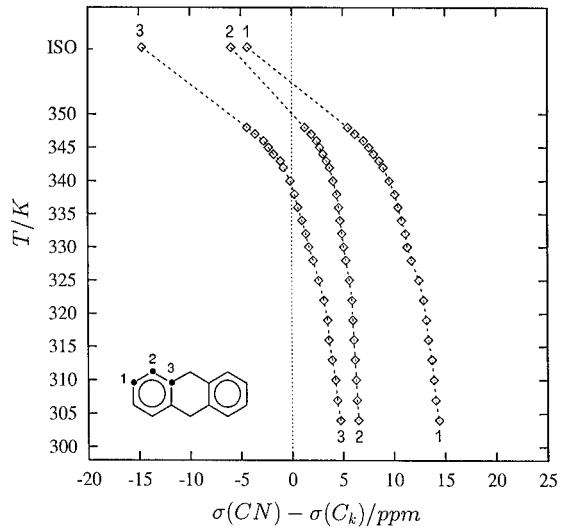

Figure 2. The same as in Figure 1, but for 9,10-dihydroanthracene (DHYA). T_{NI} = 349 K. Only the chemical shifts of the aromatic carbons are reported.

values of order parameters in I, so, for reasons of space, here we shall simply outline the main steps involved.

The observed differences $\sigma_J^{aniso} - \sigma_J^{iso}$ between chemical shifts in the nematic and isotropic phases can be expressed in terms of the shielding tensor $\boldsymbol{\sigma}_J^{MOL}$ components in a molecular fixed frame for each chemically different carbon J, for molecules with effective D_{2h} symmetry like those used in the present work, as[8]

$$\frac{\sigma_J^{aniso} - \sigma_J^{iso}}{S_f} = \left[\langle P_2\rangle \sigma_{J,ZZ}^{MOL} + \sqrt{\frac{2}{3}}\langle D_{0,2}^2\rangle(\sigma_{J;XX}^{MOL} - \sigma_{J;YY}^{MOL})\right] \quad (1)$$

where we have chosen the molecular frame as that diagonalizing the ordering tensor. $\langle P_2\rangle$, $\langle D_{02}^2\rangle$ are the orientational order parameters,[13] and S_f (−0.5 for ZLI-1167) is an angular factor related to the diamagnetic susceptivity anisotropy of the liquid crystal. More explicitly, given that the molecular frame has orientation specified by the Euler angles[14] β,γ with respect to

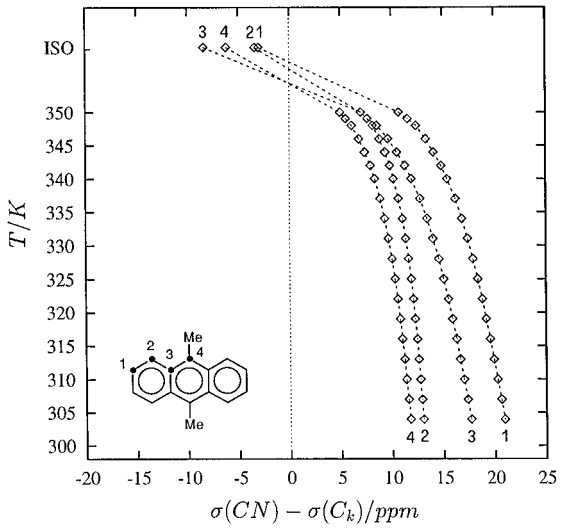

Figure 3. The same as in Figure 1, but for 9,10-dimethylanthracene (DMEA). T_{NI} = 352 K. Only the chemical shifts of the aromatic carbons are reported.

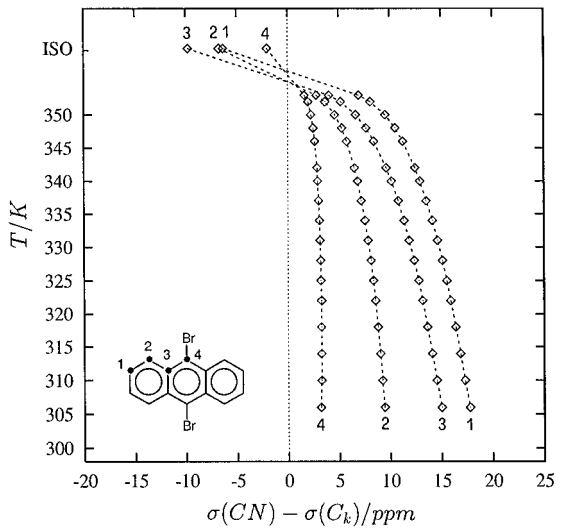

Figure 4. The same as in Figure 1, but for 9,10-dibromoanthracene (DBRA). T_{NI} = 353 K.

the director, we define $\langle P_2\rangle = \langle 3\cos^2\beta - 1\rangle/2 = S_{zz}$ and $\langle D_{02}^2\rangle = \sqrt{3/8}\langle \sin^2\beta\cos 2\gamma\rangle = (S_{xx} - S_{yy})/\sqrt{6}$, where S_{ii} are the elements of the Saupe ordering matrix[6,13] very often used in NMR work.

Alternatively, one can write the same observable in terms of the principal axis components of each of the $\boldsymbol{\sigma}_J^{MOL}$ tensors:

$$\begin{aligned}\frac{\sigma_J^{aniso} - \sigma_J^{iso}}{S_f} = &\left(\frac{3}{2}\cos^2\beta_J - \frac{1}{2}\right)\langle P_2\rangle_{T_i}\sigma_{J;33} + \\ &\frac{1}{2}\sin^2\beta_J\cos 2\gamma_J\langle P_2\rangle_{T_i}(\sigma_{J;11} - \sigma_{J;22}) + \\ &\sqrt{\frac{3}{2}}\sin^2\beta_J\cos 2\alpha_J\langle D_{02}^2\rangle_{T_i}\sigma_{J;33} + \\ &\frac{1}{\sqrt{6}}[\cos 2\alpha_J\cos 2\gamma_J(1+\cos^2\beta_J) - \\ &2\sin 2\alpha_J\sin 2\gamma_J\cos\beta_J]\langle D_{02}^2\rangle_{T_i}(\sigma_{J;11} - \sigma_{J;22}) \quad (2)\end{aligned}$$

where α_J, β_J, γ_J are the Euler angles[14] relating the molecular frame to the frame where $\boldsymbol{\sigma}_J^{MOL}$ is diagonal, with 1 labeling the least shielded axis and 3 the most shielded one.

The order parameters can be extracted from the experimental data with a rather simple procedure, provided that the shielding

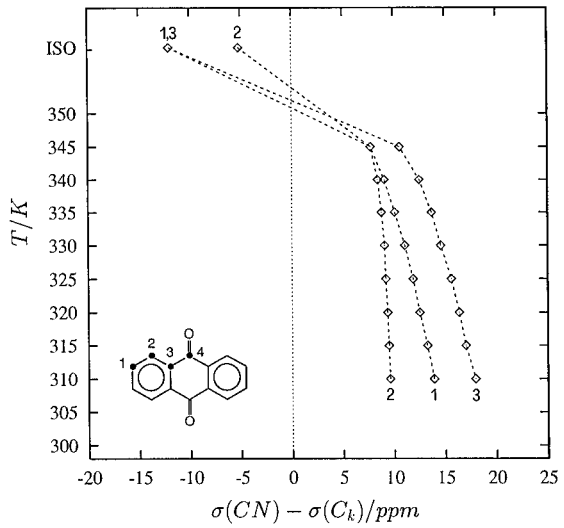

Figure 5. The same as in Figure 1, but for anthraquinone (ATQN). $T_{NI} = 354$ K. The shifts of the carbonyl carbon C(4) fall outside the scale of the graph.

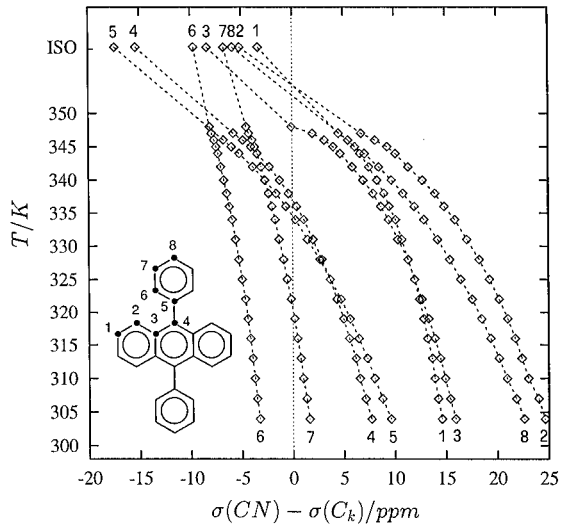

Figure 6. The same as in Figure 1, but for 9,10-diphenylanthracene (DPHA). $T_{NI} = 349$ K.

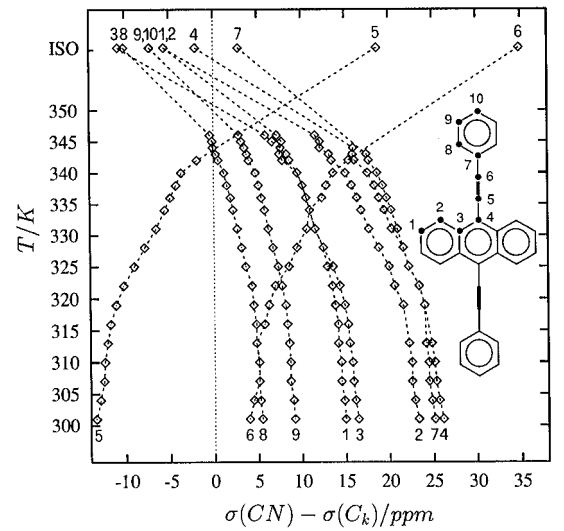

Figure 7. The same as in Figure 1, but for 9,10-bis(phenylethynyl)-anthracene (DPEA). $T_{NI} = 347$ K.

tensors $\boldsymbol{\sigma}$ are known. Unfortunately, this is not often the case, and the problem thus becomes apparently an insoluble one. Against this pessimistic view, we have demonstrated in I that

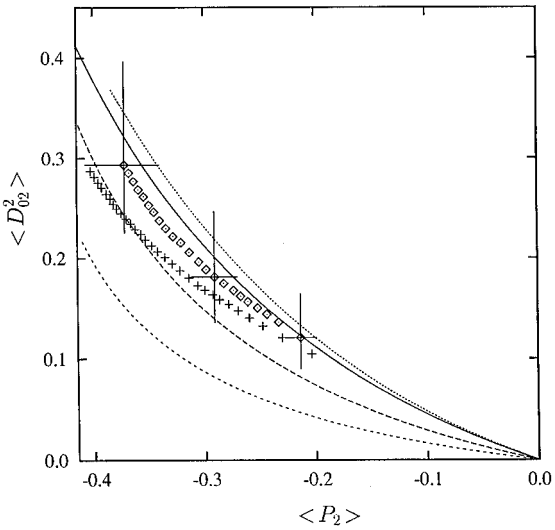

Figure 8. Orientational order parameter $\langle D^2_{02} \rangle$ plotted as function of $\langle P_2 \rangle$ for anthracene (ANTH) ($\diamond$) in ZLI1167. The error bars superimposed to the data points show the confidence interval for the order parameters, as described in section 3. The curves correspond to the theoretical order parameters calculated from LZNS (continuous), VKB (dots), FMNL (dashes), and FMNL(C) (short dashes) (see section 4). Experimental[26] order parameters from DNMR (+) are also shown.

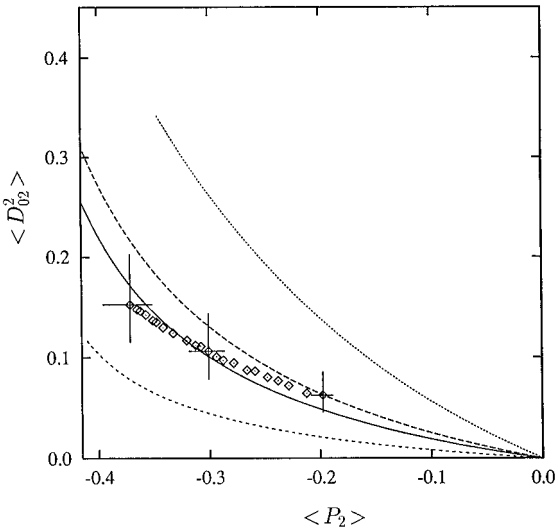

Figure 9. The same as in Figure 8, but for 9,10-dihydroanthracene (DHYA). For the analysis the molecule has been assumed in a boat conformation with a bending angle of 144.7° (see text for details).

the order parameters can be extracted if at least a small subset of chemical shift tensors can be reasonably guessed or mutuated from some similar molecular substructures as, in our case, the anthracene fragment.

The "best" set of variables among the infinite ones that satisfy the system of equations for various nuclei J in eq 2 can be obtained using an iterative procedure, starting, for molecules where the principal axis system can be located by symmetry as in the present case, from an educated guess of the shielding tensors for at least two different carbons and calculating both the molecular order parameters and the shielding constants for the remaining carbons.

In practice, once the reference carbons have been chosen and each peak in the nematic phase has been tentatively assigned (as already mentioned for the assignments in the isotropic phase, we essentially resort to literature data), the analysis proceeds in three steps.

First we calculate the trial order parameters, using only the experimental data corresponding to the carbons chosen as

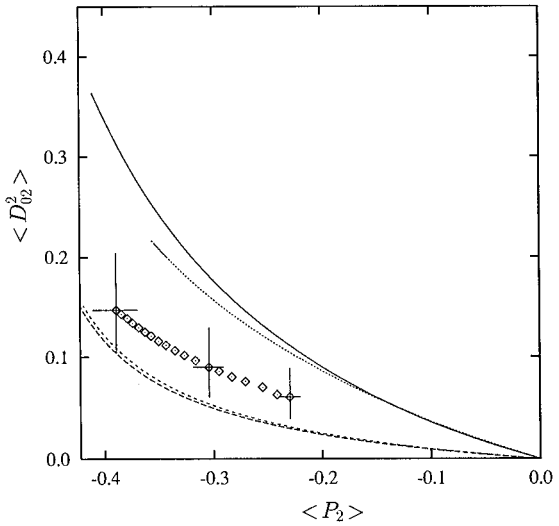

Figure 10. The same as in Figure 8, but for 9,10-dimethylanthracene (DMEA).

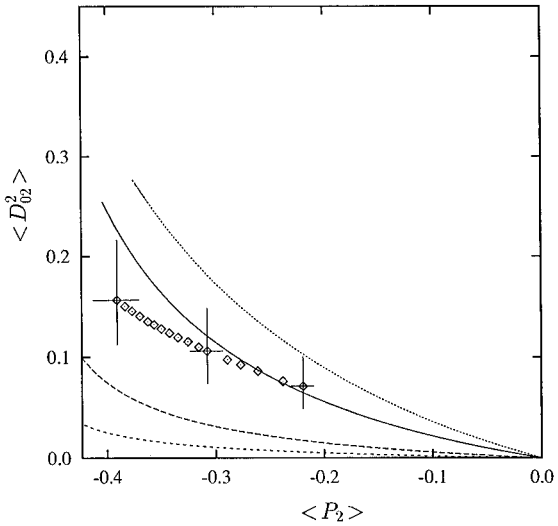

Figure 11. The same as in Figure 8, but for 9,10-dibromoanthracene (DBRA).

reference, by means of a two-dimensional linear regression to eq 2, with the shielding tensors fixed to the guessed values. We then evaluate from eq 2 the shielding tensors of the other carbons, using the remaining experimental data and fixing the order parameters to the values previously determined. Finally the order parameters are recalculated using all the experimental data and shielding tensors (guessed and calculated). The assignment of the lines in the ordered phase is checked by inspection of the residuals (difference between experimental and calculated shifts).

The final results could depend in principle on the initial guesses; nevertheless we have found that the precision of the retrieved order parameters is comparable to that attainable from DNMR,[8] while the shielding constants recovered for the unknown carbons agree at least at a qualitative and semiquantitative level with those obtained from other techniques.

As discussed in I, the selection of the subset of two or more reference carbons in the molecule under study is the most critical step of all the procedure. Here we choose to use for all the molecules the same two carbons, that is those labeled as 1,2 in all the structures, and the chemical shifts borrowed either from naphthalene[15] for the same carbons, or from benzene[16] or acetophenone[17] when the aromaticity of the middle ring is broken (DHYA and ATQN). To make the comparison easier, a common molecular frame of reference has been adopted, although it is not necessarily the one giving the minimum biaxiality for all molecules, e.g. for ANTH and DPEA. This common frame has the *z* axis perpendicular to the molecular plane of the anthracene moiety and the *x* axis parallel to its long in-plane axis.

The results of the analysis are shown in Figures 8−15, together with the values predicted by means of some theoretical models, to be discussed in the next section. Confidence level bars in Figures 8−15 have been evaluated by allowing for reference carbons a simultaneous variation of ±3 ppm on σ_{11}, σ_{22}, and σ_{33} and of ±5° on the angle γ_J defining the in-plane orientation of the principal frame.

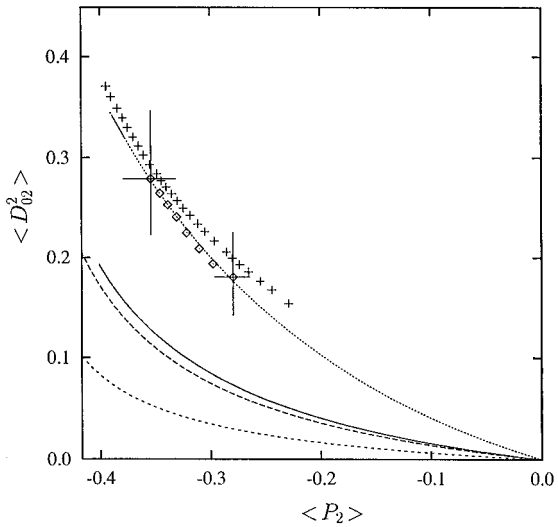

Figure 12. The same as in Figure 8, but for anthraquinone (ATQN). Experimental[36] order parameters from DNMR (+) are also shown.

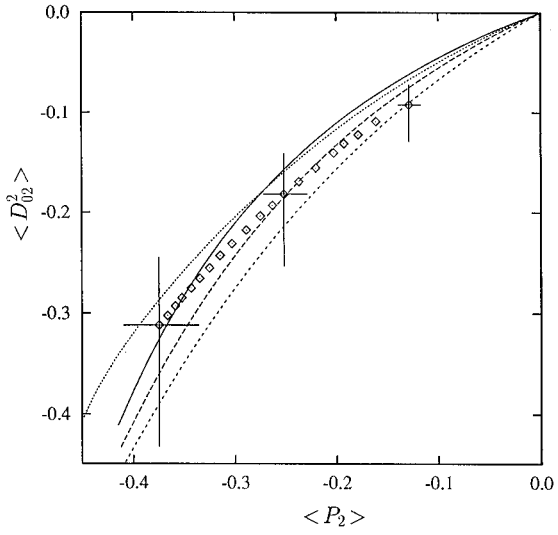

Figure 13. The same as in Figure 8, but for 9,10-diphenylanthracene (DPHA). The theoretical curves have been calculated assuming the phenyl ring twisted at 90° with respect to the anthracene moiety.

4. Theoretical Models

The interaction of a biaxial object with a uniaxial anisotropic medium is theoretically described by a number of models, mainly at molecular field level, where, in the high dilution limit, the solute interacts only with the average effective field generated by the solvent. Here we have considered only three of them: the one based on polarizability of Luckhurst et al. (LZNS),[4] the continuum elastic model of Van der Est et al. (VKB),[3] and the surface tensor model of Ferrarini et al.

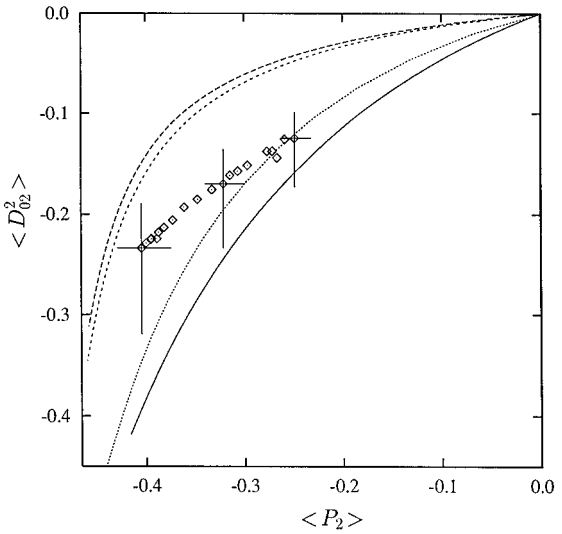

Figure 14. The same as in Figure 8, but for 9,10-bis(phenylethynyl)-anthracene. The theoretical curves have been calculated assuming the molecule planar.

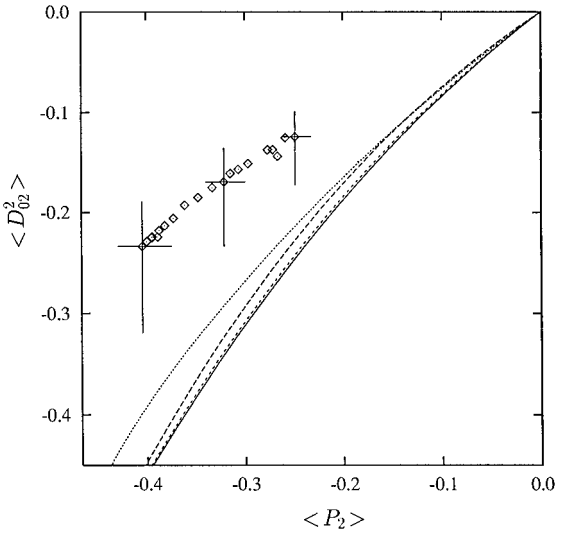

Figure 15. The same as in Figure 14, but with the theoretical curves calculated assuming the phenyl ring twisted at 90° with respect to the anthracene moiety.

(FMNL).[5] All these models define an anisotropic orienting potential $U(\beta,\gamma)/k_BT$ (k_B is the Boltzmann constant) whose biaxiality depends only on some properties of the dissolved molecule and describes the interaction between the solute and the solvent by means of a single temperature-dependent parameter ϵ. Order parameters are then calculated as Boltzmann averages:

$$\langle D^2_{0n}\rangle = \frac{\int_0^{\pi}\int_0^{2\pi} D^2_{0n}(\beta,\gamma)\exp[-U(\beta,\gamma)/k_BT]\,d\beta\sin\beta\,d\gamma}{\int_0^{\pi}\int_0^{2\pi}\exp[-U(\beta,\gamma)/k_BT]\,d\beta\sin\beta\,d\gamma}, \quad n = 0, 2 \tag{3}$$

where $U(\beta,\gamma)/k_BT$ is differently defined according to the various models.

(i) VKB.[3] In this approach the liquid crystal solvent is considered as an elastic continuum deformed as the solute changes its orientation and

$$U(\beta,\gamma)/k_BT = \epsilon[C(\beta,\gamma)]^2 \tag{4}$$

TABLE 1: Molecular Polarizabilities (Å^3), Corresponding Biaxialities λ_α Calculated with the MNDO Method, and Surface Tensor (FMNL) Biaxialities λ_S (Axes Are Oriented As Defined in Section 3)

molecule	α_{xx}	α_{yy}	α_{zz}	λ_α	λ_S
ANTH[a]	44.1	27.7	8.7	−0.370	−0.234
DHYA[b]	32.3	28.0	12.5	−0.152	−0.203
DMEA	47.3	33.9	12.4	−0.291	−0.073
DBRA	48.7	39.7	12.9	−0.176	−0.046
ATQN	35.6	30.6	8.9	−0.127	−0.111
DPHA	50.9	66.3	33.0	0.369	0.457
DPEA (planar)	68.1	113.8	17.6	0.381	0.091
DPEA (twisted 90°)	52.8	106.4	35.2	0.740	0.643

[a] Experimental values:[19] $\alpha_{xx} = 35.6$; $\alpha_{yy} = 25.0$; $\alpha_{zz} = 15.6$ Å^3; $\lambda_\alpha = -0.437$. [b] Corresponding to a bending angle of 144.7°.

where $C(\beta,\gamma)$ is the contour length of the projection of the solution molecule on the plane perpendicular to the director, evaluated according to the maximum circumference method described in ref 3.

(ii) LZNS.[4] In this case the basic solute−solvent interactions are assumed to be anisotropic dispersion forces and

$$U(\beta,\gamma)/k_BT = \epsilon[D^2_{00}(\beta) + \lambda_\alpha \,\mathrm{Re}\, D^2_{02}(\beta,\gamma)] \tag{5}$$

with the biaxiality parameter λ_α evaluated from the solute polarizability tensor $\boldsymbol{\alpha}$ according to[4,18]

$$\lambda_\alpha = \sqrt{\frac{3}{2}}\frac{\alpha_{xx} - \alpha_{yy}}{2\alpha_{zz} - \alpha_{xx} - \alpha_{yy}} \tag{6}$$

(iii) FMNL.[5] This model is based on the idea that the ordering of a solute is related to its shape, in such a way that the ordering along a certain direction is proportional to the exposed molecular surface in that direction. To quantify this, Ferrarini et al.[5] introduced a surface tensor, with spherical components

$$S^{2,m} = -\int_S D^2_{0m}(\theta,\phi)\,dS \tag{7}$$

where (θ, ϕ) is the orientation of a unit vector normal to the local surface and the integration is extended to the surface of the molecule, S, obtained by centering a van der Waals sphere on every atom or, in some cases, groups of atoms. The potential of mean torque is then written as

$$U(\beta,\gamma)/k_BT = \epsilon[D^2_{00}(\beta) + \lambda_S \,\mathrm{Re}\, D^2_{02}(\beta,\gamma)] \tag{8}$$

where λ_S is the ratio of two irreducible components of the surface tensor **S**, i.e. $\lambda_S = S^{22}/S^{20}$.

To apply the various models, we need the molecular polarizabilities for the LZNS and molecular geometries and the van der Waals radii for the VKB and FMNL calculations.

Experimental polarizabilities are available only for ANTH[19] so, to treat all the molecules at the same level of approximation, we have decided to compute all the polarizabilities at a semiempirical level by means of the MNDO method,[20] which has proved to give reasonably good results for polycyclic aromatic hydrocarbons.[21,22] The calculated polarizabilities are reported in Table 1.

As for the molecular geometries, we have evaluated them again at the semiempirical level using the PM3 method.[23] Both MNDO and PM3 are included in the program package MOPAC, version 6.[24] The van der Waals radii required to evaluate molecular shapes and surfaces have been taken from Bondi[25] and from Ferrarini et al.[5] and are reported in Table 2.

TABLE 2: Van der Waals Radii of the Atoms and Groups Used in the Computation of the Molecular Surfaces[5,25]

atom	vdW radius/Å
C (aromatic)	1.77
C (acetylenic)	1.77
C (aliphatic)	1.70
H (aromatic)	1.0
H (aliphatic)	1.20
Br	1.92
O	1.50
CH, CH_2, CH_3 groups	2.0

For the FMNL model either we have applied the recommended procedure reported in ref 5, using a single van der Waals sphere of 2 Å radius for the CH, CH_2, and CH_3 groups, or we have considered explicitly all the atomic centers of the molecule. We shall denote this last variant as FMNL(C). In both cases we have used a grid of 400 points in each angular variable for the integration over the surface.

The theoretical predictions for these simple models have been compared with the experimental order parameters obtained from the analysis of the ^{13}C NMR spectra, and in the next section we shall comment on each one. We can see in Figures 8−15 that none of the four models are completely successful in predicting the temperature dependence of the order parameters, even if it should be remarked that this way of reporting the results enhances the differences between the various models and between the experimental data obtained from different techniques.

5. Discussion

We consider each case in turn.

ANTH. Experimental results for ANTH in the same liquid crystal have been previously presented in I using a different molecular frame. In Figure 8 we report them anyway together with the results from DNMR,[26] so as to compare them with the theoretical models and to be able to use them as a sort of reference. We can see that both the deuterium results and three out of four theoretical models fall within the estimated confidence intervals (horizontal and vertical bars). Thus on one hand a good agreement between theory and experiment is found, but on the other very little discrimination on the origin of molecular alignment can be made in this case, since surface, polarizability, and elastic models converge to the same prediction.

The model that is farther from the experimental data is, in this case, the atomic resolution surface model FNML(C). This is quite surprising at first since we might expect that putting more details into the model would improve it. However we shall see that these discrepancies are systematic in the series we have studied; that is, FNML(C) always underestimates the biaxiality of the molecule, while FNML may over- or underestimate it, but in general falls closer to the experiment.

DHYA. This molecule is rather interesting since its overall shape is, at least at first sight, fairly similar to that of ANTH, while its electronic structure is clearly different. The actual shape could however be quite different since the molecule has a torsional degree of freedom with a very flat potential energy surface,[27] which makes a boat conformation, with a bending angle of 144.7°, to be the favorite one in the crystal.[28] In solution, the preferred conformation has not been established yet, but a very fast boat-to-boat interconversion has been proposed to explain the features of the proton NMR spectrum at low temperatures.[29]

Our ^{13}C experiment is not able to discriminate between a single linear D_{2h} structure and a fast interconversion between two identical C_{2v} conformations since each half of the molecule generates identical observables. Thus, all we can determine is the average orientation of the benzene moiety with respect to the external field. To relate this information to the orientation of the whole molecule, we need to assume a particular conformation. For the purpose of analysis we have then taken the molecule bent in a boat (C_{2v}) conformation, with a bending angle equal to that in the crystal at all temperatures. The molecular z axis coincides with the C_2 axis, while the y axis is parallel to the line connecting the carbons in the 9,10 position. With this selection of the frame, the normals to the planes of the benzene moieties make an angle of 17.7° with respect to the molecular z axis. In addition, as the hydrogenation of the middle ring breaks its aromaticity, it seemed to us more appropriate to use the shielding tensor of benzene[16] for the reference carbons C(1), C(2). The temperature dependence of the chemical shifts is again described by eq 1 since the lowering of the symmetry does not introduce additional order parameters.[13]

The plausibility of all these assumptions is supported by the values obtained for the shielding tensor of carbon C(3) (see Table 3, entry b), which is found to be almost the same as the methylated carbon in *p*-xylene ($\sigma_{11} = 99$, $\sigma_{22} = 29$, $\sigma_{11} = -127$ ppm[30]).

We mention that the observed chemical shifts can be equally well analyzed by assuming a fully planar conformation, and in that case considerably lower order parameters (about 25% smaller) are obtained. Thus the order parameters shown in Figure 9 are in this case heavily biased by the assumed molecular conformation, and comparisons with the other molecules reported here should be made with caution. Given this caveat, the molecule has of course been assumed to be bent as in the crystal also for the calculations of the molecular biaxiality. As we can see from Table 1, on the basis of the surface model ANTH and DHYA should behave almost in the same way. Actually we have found that the $\langle D^2_{02}\rangle$ is much lower than for ANTH, and in this case both FMNL and LZNS models are in good agreement with experiment, while the continuum model gives the worst prediction.

DMEA. Examining Figure 10, we see that, as expected, the addition of two methyl groups in the 9,10 positions of ANTH lowers the biaxiality of the molecule, but less than predicted by the surface model. Indeed the experimental $\langle D^2_{02}\rangle$ values are only slightly lower compared to that of DHYA. The shielding tensor components of the methylated carbon result to be somewhat different from those of the corresponding carbons in *p*-xylene[30] and are closer to those of 1,4,5,8-tetramethylnaphthalene.[31] In particular, while σ_{22} does not change, σ_{11} and σ_{33} are both reduced by ∼20 ppm. On the other hand, the reliability of the values chosen for the tensor of the reference carbons C(1), C(2) is also confirmed by the values recovered for the shielding tensor components of C(3), which are very similar to those of anthracene and those typical for bridge carbons in polycyclic aromatic compounds.[15,32] In this case none of the models estimate the biaxiality within the experimental error.

DBRA. We comment first on the shielding tensors, and we notice that presently the shielding tensor of aromatic carbons carrying a bromine atom attached are not well characterized. Indeed we could find only two references in the literature. Fung and Kong found, for this type of carbon in bromobenzene,[33] $\sigma_{11} = 110.7$, $\sigma_{22} = -40.3$, $\sigma_{33} = -70.3$ ppm, while Sardashti and Maciel reported $\sigma_{11} = 86.4$, $\sigma_{22} = 26.4$, $\sigma_{33} = -112$ ppm in 1-bromo-4-cyanobenzene.[34] Our values (see Table 3, entry d) are somewhat different from both, but confirm that the least

TABLE 3: Summary of the ^{13}C Shielding Tensors Used in the Analysis of the ^{13}C NMR Spectra (Values Enclosed in Parentheses Are Recovered from the Analysis (See Text))

molecule	comments		C(1)	C(2)	C(3)	C(4)	C(5)	C(6)	C(7)	C(8)	C(9)
a	shielding tensor for carbons	σ_{11}	101.9	94.7	(75.4)	(80.5)					
	C_1, C_2 taken from naphthalene[15]	σ_{22}	13.1	13.4	(61.8)	(15.7)					
ANTH		σ_{33}	−115.0	−108.1	(−137.2)	(−96.2)					
		α	0.0	0.0	0.0	0.0					
		β	0.0	0.0	0.0	0.0					
		γ	36.0	79.0	0.0	90.0					
b	shielding tensor for carbons	σ_{11}	104.0	104.0	(95.2)						
	C_1, C_2 taken from benzene[16]	σ_{22}	16.0	16.0	(33.9)						
DHYA		σ_{33}	−120.0	−120.0	(−129.1)						
		α	0.0	0.0	0.0						
		β	0.0	0.0	0.0						
		γ	30.0	90.0	30.0						
c	shielding tensor for carbons	σ_{11}	101.9	94.7	(68.6)	(79.3)					
	C_1, C_2 taken from naphthalene[15]	σ_{22}	13.1	13.4	(64.6)	(29.0)					
DMEA		σ_{33}	−115.0	−108.1	(−133.2)	(−108.6)					
		α	0.0	0.0	0.0	0.0					
		β	0.0	0.0	0.0	0.0					
		γ	36.0	79.0	0.0	90.0					
d	shielding tensor for carbons	σ_{11}	101.9	94.7	(67.7)	(86.9)					
	C_1, C_2 taken from naphthalene[15]	σ_{22}	13.1	13.4	(56.1)	(−23.5)					
DBRA		σ_{33}	−115.0	−108.1	(−123.8)	(−63.4)					
		α	0.0	0.0	0.0	0.0					
		β	0.0	0.0	0.0	0.0					
		γ	36.0	79.0	0.0	90.0					
e	shielding tensor for carbons	σ_{11}	102.4	10.3	(128.1)	(96.4)					
	C_1, C_2 taken from acetophenone[17]	σ_{22}	17.4	29.3	(13.9)	(19.5)					
ATQN		σ_{33}	−119.8	−129.3	(−142.1)	(−115.9)					
		α	0.0	0.0	0.0	0.0					
		β	0.0	0.0	0.0	0.0					
		γ	30.0	87.0	34.0	0.0					
f	shielding tensor for carbons	σ_{11}	101.9	94.7	(63.3)	(68.0)	(−96.8)	(−60.0)	(−65.3)	(−10.5)	
	C_1, C_2 taken from naphthalene[15]	σ_{22}	13.1	13.4	(65.5)	(28.6)	(−7.8)	(32.2)	(39.2)	(−9.6)	
DPHA		σ_{33}	−115.0	−108.1	(−128.8)	(−96.6)	(−104.5)	(27.9)	(26.0)	(110.1)	
		α	0.0	0.0	0.0	0.0	0.0	0.0	0.0	0.0	
		β	0.0	0.0	0.0	0.0	0.0	0.0	0.0	0.0	
		γ	36.0	79.0	0.0	90.0	0.0	0.0	0.0	0.0	
g	shielding tensor for carbons	σ_{11}	101.9	94.7	(72.5)	(99.3)	(84.2)	(69.8)	(24.0)	(37.5)	(39.7)
	C_1, C_2 taken from naphthalene[15]	σ_{22}	13.1	13.4	(65.8)	(−12.8)	(36.2)	(52.7)	(66.6)	(39.0)	(40.8)
DPEA		σ_{33}	−115.0	−108.1	(−138.3)	(−86.5)	(−120.5)	(−122.5)	(−90.6)	(−76.4)	(−80.5)
		α	0.0	0.0	0.0	0.0	90.0	90.0	0.0	0.0	0.0
		β	0.0	0.0	0.0	0.0	90.0	90.0	0.0	0.0	0.0
		γ	36.0	79.0	0.0	90.0	0.0	0.0	0.0	0.0	0.0

shielded axis is perpendicular to the aromatic ring and the most shielded one is along the C−Br bond. Moreover, Fung and Kong found that the presence of bromine has a large long-range effect on the neighbor carbons (up to two C−C bonds away from the C−Br bond), while Sardashti and Maciel found that this effect is much less pronounced in both size and range. In this case we found that the σ_{33} component of C(3) in DBRA is about 20 ppm greater than the value typical for such kind of atom, but σ_{11} and σ_{22} are almost equal, as in ANTH and DMEA. This last point and the lack of conclusive literature data encouraged us in employing the shielding tensor of naphthalene for reference carbons C(1), C(2). But we point out that our assumption would benefit from some additional support, compared to the other molecules reported here. With this caveat we notice that the various models predict rather different biaxialities and that only the polarizability-based one is in reasonably fair agreement with the experimental data.

ATQN. This molecule has a low solubility in the liquid crystal, so very long experiments were required to achieve a sufficient signal to noise ratio. Even with this precaution the spectra close to the transition temperature were poorly defined, and they could not be reliably analyzed. As for DHYA, the molecule is not fully aromatic, so we have chosen to use for the reference carbons C(1), C(2) the shielding tensors borrowed from acetophenone,[17] instead of benzene or naphthalene. The resulting order parameters are reported in Figure 12 and compared to those obtained from DNMR.[36] The very good agreement of the two series of data supports unambiguously our assumptions. The shielding tensor for the carbonyl is found to be in close agreement with the values reported for similar compounds[17,35] (acetophenone, $\sigma_{11} = 80.7$, $\sigma_{22} = 33.7$, $\sigma_{33} = -114.7$ ppm; benzophenone, $\sigma_{11} = 72$, $\sigma_{22} = 29$, $\sigma_{33} = -101$ ppm). Comparing once more the theoretical predictions, the VKB model is the only one in excellent agreement with the experiment.

DPHA. Unlike the previous molecules, the experimental and also theoretical values of $\langle D^2_{02} \rangle$ are negative and quite large, indicating that the molecular *y* axis aligns far better than the *x* one. Indeed, by choosing a more convenient molecular frame, with the *z* axis along the short axis of anthracene and the *y* axis perpendicular to the anthracene plane, the ordering matrix changes dramatically, showing that DPHA behaves as a nearly uniaxial rod-like molecule. This is in excellent agreement with the order parameter $\langle P_2 \rangle$ obtained from fluorescence depolarization experiments at various temperatures,[37] where on the other hand a null value of $\langle D^2_{02} \rangle$ was assumed for the analysis.

Going more into detail, we notice that this molecule possesses two internal degrees of freedom, corresponding to the rotation of the two phenyls around the molecular *y* axis. However, due to sterical hindrance, the planar conformation is not favored and the molecule could even be treated as rigid with the phenyl rings nearly perpendicular to the anthracene fragment.[38] In the analysis of our spectral data we have not assumed, at first, a twisted molecular conformation. Thus we have taken the principal frame of the phenyl carbons coincident with the molecular frame (that is $\alpha = 0$, $\beta = 0$, $\gamma = 0$). This leads to the shielding tensors listed in Table 3, entry f, with the most shielded component of all the phenyl carbons along the molecular *x* axis. Although this finding is not a direct proof that the phenyls lie perpendicular to the anthracene moiety, it certainly supports the hypothesis of nonplanarity of the molecule. We shall comment in more detail when dealing with DPEA. The other two carbons, C(3) and C(4), of the anthracene fragment behave quite regularly, with the σ_{11}, σ_{22} components of the bridging C(3) carbon almost equal, as found in ANTH, DMEA, and DBRA, and the σ_{22}, σ_{33} of C(4) very similar to those previously found in ANTH and DMEA. The σ_{11} component is about 10 ppm lower than in the previous cases, but this can be attributed to a substituent effect.

DPEA. Due to incomplete proton decoupling, only 9 of the 10 different carbons are detected for DPEA in the nematic mesophase. After some checks the missing line was attributed to carbon 10, but in any case the lack of this line is not essential in the analysis.

It is interesting to note in Figure 7 that the behavior of the acetylenic carbons is markedly different from the others, shifting to lower fields as the temperature decreases. This can be rationalized in this way. For acetylenic carbons the most shielded tensor component lies along the CC triple bond. Due to the diamagnetic susceptivity anisotropy of the mesophase and the shape of the molecule, this bond tends to be aligned perpendicularly to the magnetic field, so the acetylenic carbons tend to be progressively deshielded as the order increases. This observation is rather general and could be useful to assign acetylenic carbons in other probe molecules.

The shielding tensors for the acetylenic carbons are in nice agreement with literature data,[39] with the most shielded axis aligned with the CC triple bond and the other two components almost equal. However for the acetylenic carbon C(5) the σ_{11} and σ_{22} components differ more than the error threshold expected from this method, so the observed anisotropy can be attributed only to an effect of the anthracene fragment.

For this molecule we found some disagreement between our findings and the literature assignments of the nonprotonated carbons in the isotropic phase. In fact, using the literature assignment,[11] we recover for carbons C(3), C(4), C(5), C(7) shielding tensors very different from the expected ones, while with our proposal all the inconsistencies are removed. Thus we believe our assignment to be the correct one. Indeed, as stated by the authors in ref 11, their assignment of nonprotonated carbons was only tentative.

As for DPHA, this molecule cannot be considered rigid. From PM3 calculations the energy of the twisted form with the phenyl at 90° with respect the anthracene fragment plane is predicted to be only 0.8 kcal/mol above the planar form, so in principle the phenyl rings may be nearly freely rotating. If we assume, for the purpose of analysis, the principal frame of the phenyl carbons to be coincident with the molecular frame, we recover the shielding components listed in Table 3, entry g. In this case we found the $\sigma_{33} \equiv \sigma_{ZZ}^{MOL}$ components be the most shielded ones, while a free rotation of the phenyls around the C(6)−C(7) bond in the time scale of the experiment would have produced equal σ_{XX}^{MOL}, σ_{ZZ}^{MOL}. This suggests that in the liquid crystal the molecule adopts a preferred conformation with the anthracene and phenyl moieties nearly coplanar.

A rather crude estimate of the torsional angle between the phenyls and the anthracene fragments in DPHA and DPEA has been obtained by assuming for the carbons C(6), C(7) of DPHA and C(8), C(9) of DPEA the shielding tensor of benzene and fitting the angle β between ring and molecule axis in order to reproduce (see eqs 7.a and 7.b in ref I) the σ_{XX}^{MOL}, σ_{YY}^{MOL}, σ_{ZZ}^{MOL} recovered for these carbon from the analysis (Table 3, entries f, g). The angles α and γ have been kept fixed to 0° and 30°, respectively, in order to maintain σ_{33} perpendicular to the phenyl ring and σ_{11} along the CH bond.

The fitting procedure gives a twist angle β of 58° for DPHA and 27° for DPEA. If these values of β, together with $\alpha = 0°$ and $\gamma = 30°$, are introduced in eq 2 and the whole analysis is repeated, they produce the following values for the shielding tensors of C(6), C(7) and C(8), C(9), for DPHA and DPEA, respectively: C(6) (DPHA) $\sigma_{11} = 108.1$, $\sigma_{22} = 6.9$, $\sigma_{33} = -115.0$ ppm; C(7) (DPHA) $\sigma_{11} = 105.0$, $\sigma_{22} = 17.3$, $\sigma_{33} = -122.3.0$ ppm.; C(8) (DPEA) $\sigma_{11} = 98.8$, $\sigma_{22} = 19.0$, $\sigma_{33} = -117.8$ ppm; (C9)(DPEA) $\sigma_{11} = 104.5$, $\sigma_{22} = 19.6$, $\sigma_{33} = -124.1$ ppm, showing that the procedure is at least consistent. All these tensors are very close to the shielding tensor of benzene (we recall that for benzene $\sigma_{11} = 104.0$, $\sigma_{22} = 16.0$, $\sigma_{33} = -120.0$ ppm[16]), thus confirming *a posteriori* the validity of the assumptions made to perform the conformational analysis.

A torsion angle of ∼58° for DPHA is not surprising, since the sterical hindrance of the phenyl practically forbids this molecule to assume a planar conformation and the agreement with the value of 67.6° found in the crystal[38] is noteworthy. On the other hand, the same procedure applied to DPEA retrieves a torsion angle for the phenyl of ∼27° that cannot be accounted for by simple sterical arguments (we recall that semiempirical PM3 calculations on the isolated molecule find an energy difference less than 1 kcal/mol between the planar and the 90° twisted structures); thus other mechanisms, such as interactions with the solvent, should be invoked.

It is also interesting to note (cf. Figures 14, 15) that the theoretical models are in somewhat better agreement with the planar conformation. Thus, even though no one exactly agrees with experiment, the observed biaxial orders are bound by the different predictions in the planar case, while they are consistently different in the 90° twisted case. In the case of DPEA, as for DPHA, the molecule behaves more like a distorted rod.

6. Conclusions

We have applied a recently proposed technique[8] based on the analysis of temperature-dependent ^{13}C NMR spectra to the determination of the orientational order parameters of anthracene and of six of its 9,10 derivatives dissolved in the nematic liquid crystal mixture ZLI-1167. The results have been compared with the predictions of some simple mean field theoretical models. We have found that none of them are fully successful in predicting the temperature dependence of the order parameters. In particular the shape-based elastic model of Burnell and coworkers (VKB)[3] tends to systematically overestimate the molecular biaxiality, while the polarizability model of Luckhurst et al. (LZNS)[4] and the surface tensor model of Ferrarini et al. (FMNL)[5] give predictions that, on average, fall closer to the experimental points. A variant of the FMNL model, including atomic details, proved to give poorer results since it always underestimated the experimental molecular biaxiality. The reason could be in the fact that the surface tensor of a sphere

or of an arbitrary collection of tangent spheres is zero and that adding more atomic details could somehow approach this situation.

Even at this approximate level the mean field models can be quite useful to aid spectral analysis. For instance the LZNS model was used to perform a simulation of the ^{13}C spectra of DPEA, which proved to be very helpful in the assignments of the corresponding experimental spectra. As for the more ambitious goal of a prediction of the ordering matrix from scratch, we think that these models can only be useful to get a rough estimate of the temperature dependence of the order parameters.

From the analysis of the ^{13}C NMR spectra it is also possible to recover with reasonable accuracy the shielding tensors of all the unequivalent carbons of the probe molecule. These results compare well with literature data where available.

Acknowledgment. We are grateful to MURST, CNR, and EEC HCM for financial support. We are particularly indebted to Dr. A. Hagemeyer, Mr. D. Macciantelli (ICOCEA, CNR), and to Dr. D. Casarini for their help with the experiments and to Prof. L. Lunazzi for the use of the CXP300 spectrometer. We also wish to thank Dr. A. Ferrarini and Prof. P. L. Nordio for a copy of their surface tensor model program and Prof. D. J. Photinos for a useful conversation.

References and Notes

(1) See, for example: Bahadur, B., Ed. *Liquid Crystals, Application and Uses*; World Scientific: Singapore, 1990. See also: McEwen, R. S. *J. Phys. E: Sci. Instrum.* **1987**, *20*, 364.

(2) (a) Michl, J.; Thulstrup, E. W. *Spectroscopy with Polarized Light*; VCH: New York, 1987. (b) Samorí, B.; Thulstrup, E. W., Eds. *Polarized Spectroscopy of Ordered Systems*; Kluwer: Dordrecht, 1988.

(3) Van der Est, A. J.; Kok, M. Y.; Burnell, E. E. *Mol. Phys.* **1987**, *60*, 397.

(4) Luckhurst, G. R.; Zannoni, C.; Nordio, P. L.; Segre, U. *Mol. Phys.* **1975**, *30*, 1345.

(5) Ferrarini, A.; Moro, G. J.; Nordio, P. L.; Luckhurst, G. R. *Mol. Phys.* **1992**, *77*, 1.

(6) Emsley, J. W.; Lindon, J. C. *NMR Spectroscopy Using Liquid Crystals*; Pergamon: Oxford, 1975.

(7) Emsley, J. W., Ed. *Nuclear Magnetic Resonance of Liquid Crystals*; Reidel: Dordrecht, 1985.

(8) Hagemeyer, A.; Tarroni, R.; Zannoni, C. *J. Chem. Soc., Faraday Trans.* **1994**, *90*, 3433.

(9) (a) Wedel, H.; Haase, W. *Chem. Phys. Lett.* **1978**, *55*, 96. (b) Pohl, L.; Eidenschink, R.; Krause, J.; Weber, G. Presented at the 7th International Liquid Crystals Conference, Bordeaux, 1978. (c) MERCK data sheets.

(10) Bremser, W.; Ernst, L.; Franke, B.; Gerhards, R.; Hardt, A. *Carbon-13 NMR Spectral Data*; Verlag Chemie: Weinheim, 1981.

(11) Hirayama, M.; Kobayashi M.; Yamamoto, H. *Bull. Chem. Soc. Jpn.* **1988**, *61*, 1501.

(12) Storek, W.; Sauer, J.; Stösser, R. *Z. Naturforsch.* **1979**, *34a*, 1334.

(13) Zannoni, C. In *The Molecular Physics of Liquid Crystals*; Luckhurst, G. R., Gray, G. W., Eds.; Academic Press: New York, 1979; Chapter 3, p 51.

(14) Rose, M. E. *Elementary Theory of Angular Momentum*; Wiley: New York, 1957.

(15) Sherwood, M. H.; Facelli, J. C.; Alderman, D. W.; Grant, D. M. *J. Am. Chem. Soc.* **1991**, *113*, 750.

(16) Strub, H.; Beeler, A. J.; Grant, D. M.; Michl, J.; Cutts, P. W.; Zilm, K. W. *J. Am. Chem. Soc.* **1983**, *105*, 3333.

(17) Van Dongen Torman, J.; Veeman, W. S.; De Boer, E. *J. Magn. Reson.* **1978**, *32*, 49.

(18) Catalano, D.; Forte, C.; Veracini, C. A.; Zannoni, C. *Isr. J. Chem.* **1983**, *23*, 283.

(19) Ruessink, B. H.; MacLean, C. *J. Chem. Phys.* **1986**, *85*, 93.

(20) (a) Dewar, M. J. S.; Thiel, W. *J. Am. Chem. Soc.* **1977**, *99*, 4899. (b) *Ibid.* **1977**, *99*, 4907.

(21) Dewar, M. J. S.; Steward, J. J. P. *Chem. Phys. Lett.* **1984**, *111*, 416.

(22) Lu, Y.-J.; Lee, S.-L. *Chem. Phys.* **1993**, *179*, 431.

(23) Steward, J. J. P. *J. Comput. Chem.* **1989**, *10*, 221.

(24) *MOPAC. A General Molecular Orbital Package* (QCPE program no. 455); The Quantum Chemistry Program Exchange, Department of Chemistry, Indiana University: Bloomington, 1990.

(25) Bondi, A. *J. Phys. Chem.* **1964**, *68*, 441.

(26) Emsley, J. W.; Hashim, R.; Luckhurst, G. R.; Shilstone, G. M. *Liq. Cryst.* **1986**, *1*, 437.

(27) Schaefer, T.; Sebestian, R. *J. Mol. Struct. (THEOCHEM)* **1987**, *153*, 55.

(28) Herbstein, F. H.; Kapon, M.; Reisner, G. M. *Acta Crystallogr., Sect. B* **1986**, *42*, 181.

(29) Rabideau, P. W. *Acc. Chem. Res.* **1978**, *11*, 141.

(30) Van Dongen Torman, J.; Veeman, W. S. *J. Chem. Phys.* **1978**, *68*, 3233.

(31) Orendt, A. M.; Sethi, N. K.; Facelli, J. C.; Horton, W. J.; Pugmire, R. J.; Grant, D. M. *J. Am. Chem. Soc.* **1992**, *114*, 2832.

(32) Carter, C. M.; Alderman, D. W.; Facelli, J. C.; Grant, D. M. *J. Am. Chem. Soc.* **1987**, *109*, 2639.

(33) Fung, B. M.; Kong, C. F. *J. Am. Chem. Soc.* **1984**, *106*, 6193.

(34) Sardashti, M.; Maciel, G. E. *J. Phys. Chem.* **1988**, *92*, 4620.

(35) Kempf, J.; Spiess, H. W.; Hauerlen, U.; Zimmerman, H. *Chem. Phys. Lett.* **1972**, *17*, 39.

(36) Shilstone, G. N. Ph.D. Thesis, Southampton, 1986.

(37) Arcioni, A.; Tullio, A.; Zannoni, C. Manuscript in preparation.

(38) Becker, H.-D.; Langer, V.; Sieler, J.; Becker, H.-C. *J. Org. Chem.* **1992**, *57*, 1883.

(39) Pines, A.; Gibby, M. G.; Waugh, J. S. *Chem. Phys. Lett.* **1972**, *15*, 313.

JP962052+